Fibonacci Sequence–Based Design and Analysis of Stable Second-Order LTI Systems

Abstract

Fibonacci sequence, known for its mathematical elegance & recurrence properties, brings a novel approach to filter design. In this paper we aim to design 2nd order linear time invariant (LTI) systems using pairs of consecutive higher order Fibonacci numbers. The analyses of designed systems for their overall stability i.e in terms of Routh-Hauritz criterion , gain and phase margins reveal that all the designed transfer function are stable. The impulse response represents Dirac delta function and the step response is slightly over damped with damping ratio $\zeta \approx 1.029$. The magnitude response is similar to that of a low pass filter. Monte Carlo Simulations to predict their cut off frequency validates the theoretical analysis. We have showed that the cut off frequency is 0.618 times the square root of the product of Fibonacci pairs.

Keyword: Fibonacci series, LTI system,bode plot, step response,Monte Carlo simulation

1. Introduction

The elegance of the Fibonacci sequence has emerged as powerful applications spanning science, information technology, and engineering disciplines [1, 2, 3, 4].

Recent advances in filter design have explored the unique properties of Fibonacci sequences to construct stable and selective low-pass filters, as demonstrated in both analog and photonic domains [5, 6, 7]. Theoretical advances have refined polynomial models combining Fibonacci and Lucas structures, enhancing analytical treatment of transfer functions [8]. Furthermore, interdisciplinary studies highlight biological systems exhibiting filtering characteristics influenced by Fibonacci sequences, potentially inspiring novel bio-electronic designs [9]. Beyond engineering, the Fibonacci sequence also apprise design principles in art and architecture through golden ratio-based aesthetic patterns [10, 11].

Simulation by Scilab in implementation and analysis in terms of bode plot, impulse and step responses [12], design of higher order filter using LTspice software [13] and designing filter of Sallen-Key topology with Butterworth response by Circuit Maker & MATLAB [14, 15] are studied and effectiveness of the software programs are established. Paper [16] proposed and simulated a RF active band pass filter from a transfer function. [17]suggest the detection of the pole zero position without practically going through the working of the filter.

Few literature are found in which author have designed filter using Fibonacci sequence. [18] explained the design of filter bank from Fibonacci sequence.

The authors aim on linking mathematical sequence to filter design. Designing a stable transfer function with large gain margin from the sequence is the primary task in this field which is still unexplored.Linking the recurrence relation to the coefficients of characteristic equation of a transfer function is quite creative. In this pursuit,the authors attempt to use recurrence relation of Fibonacci sequence to design a transfer function.

2. Theory

The general expression of 2nd order transfer function with unit dc gain in terms of natural frequency ω_n and damping ratio ζ is

$$T(s) = \frac{v(s)}{u(s)} = \frac{\omega_n^2}{s^2 + 2\zeta\omega_n s + \omega_n^2}, \tag{1}$$

with dc gain "1" and damping frequency

$$\omega_d = \omega_n\sqrt{(1-\zeta^2)} \tag{2}$$

At $-3dB$ point the gain is $\frac{1}{\sqrt{2}}$ times of the dc gain. For cut off frequency

$$|T(j\omega_c)| = \frac{1}{\sqrt{2}}|T(j0)|,$$

where

$$\begin{aligned} |T(j\omega)| = &\quad \frac{\omega_n^2}{\sqrt{(\omega_n^2-\omega^2)^2 + (2\zeta\omega_n\omega)^2}} \\ \phi = &\quad tan^{-1}\left[\frac{2\zeta\omega_n\omega}{(\omega_n^2-\omega^2)}\right] \end{aligned}$$

With $s = j\omega = 0, |T(j0)| = 1$ in our model of the LTI, the general expression of cut off frequency ω_c is

$$\frac{\omega_n^2}{\sqrt{(\omega_n^2-\omega_c^2)^2 + (2\zeta\omega_n\omega_c)^2}} = \frac{1}{\sqrt{2}}.1 \tag{3}$$

Squaring and rearranging we get

$$\begin{aligned} \omega_c^4 + 2\omega_n^2\omega_c^2(2\zeta^2-1) - \omega_n^4 = 0 \\ \left[\omega_c^2 + \omega_n^2(2\zeta^2-1)\right]^2 - \omega_n^4\left[(2\zeta^2-1)^2+1\right] = 0 \end{aligned}$$

Substituting $(2\zeta^2 - 1 = A)$, we write

$$\begin{aligned} [\omega_c^2 + \omega_n^2 A]^2 - [\omega_n^2\sqrt{A^2+1}]^2 = 0 \\ (\omega_c^2 + \omega_n^2.A + \omega_n^2\sqrt{A^2+1})(\omega_c^2 + \omega_n^2.A - \omega_n^2\sqrt{A^2+1}) = 0 \\ \omega_c^2 = -\omega_n^2[A + \sqrt{A^2+1}], \qquad \omega_n^2(\sqrt{A^2+1} - A) \end{aligned}$$

Considering the positive value and substituting for A the general expression of cut off frequency is

$$\omega_c = \omega_n \sqrt{1 - 2\zeta^2 + \sqrt{4\zeta^4 - 4\zeta^2 + 2}} \tag{4}$$

Depending on the values of ζ and ω_n the transfer function has different responses and cut of frequencies (-3dB point).

3. Method

We started with the general form of second order transfer function in terms of natural frequency ω_n and damping factor ζ and theoretically analyse it to calculate the cut off frequency,the impulse and step responses for different values of ζ. Now we design a model second order transfer function in the form of,

$$T(s) = \frac{p_1 p_2}{(s - p_1)(s - p_2)}$$

where p_1 and p_2 are poles to be replaced by two consecutive Fibonacci numbers in golden ratio. To ensure that the poles locate in the left hand side of s-plan we use a negative sign with the Fibonacci numbers. The transfer function now takes the form as in equation (5) which is in conformity with equation (1).

$$T(s) = \frac{fib1.fib2}{s^2 + (fib1 + fib2)s + fib1.fib2} \tag{5}$$

Equation (1) gives

$$\begin{aligned} 2\zeta\omega_n &= fib1 + fib2 \\ \omega_n^2 &= fib1.fib2 \\ \zeta &= \frac{fib1+fib2}{2\sqrt{fib1.fib2}} \end{aligned} \tag{6}$$

We select values of (fib1,fib2) from (21,34),(34,55),(55,89),(89,144),... to (46386, 750250) such that $\frac{fib2}{fib1} \approx 1.618$. The ζ values given by equation (6) lie in the range from 1.029161634 to 1.029085514 for those pairs and for pairs (89-144) onwards the ζvalue is 1.029085 and they all represent over-damped system.

From the design methodology of the transfer function, they are stable from pole position. Still they are further subjected to Routh-Houritz (RH) criterion and array.

Impulse responses & step responses are drawn using Scilab 6.1.1. We apply Monte Carlo simulation to the transfer functions with randomness of ζ. In equation (6), we choose 5% variation of the numerator and denominator for 100 random ζ values in normal distribution.Using

$$\frac{d\zeta}{\zeta} = \frac{d(fib1 + fib2)}{(fib1 + fib2)} + \frac{1}{2}\frac{d(fib1.fib2)}{(fib1.fib2)}$$

$$\frac{d\zeta}{\zeta} = \frac{7.5}{100} \tag{7}$$

clearly, $d\zeta = 7.5\%.\zeta$. A normal distribution of ζ in the range from 1.029085 to 1.106 is used as input. A python program is iterated 100 times in Monte Carlo Simulation, using Spyder 6, a python IDE to draw bode plot and calculate the cut off frequency. the python program also calculate the mean cut of frequency with standard deviation. We also perform z-test to validate the analytically calculated

cut off frequency.

4. Result

Now we design first six transfer functions as prototype with the first six pairs of Fibonacci number (89,144),(144,233),(233,377),(377,610),(610,987) and (987,1587).

$$\begin{aligned} T_1(s) &= \frac{89.144}{s^2+(89+144)s+89.144} \\ T_2(s) &= \frac{144.233}{s^2+(144+233)s+144.233} \\ T_3(s) &= \frac{233.377}{s^2+(233+377)s+233.377} \\ T_4(s) &= \frac{377.610}{s^2+(377+610)s+377.610} \\ T_5(s) &= \frac{610.987}{s^2+(610+987)s+610.987} \\ T_6(s) &= \frac{987.1597}{s^2+(987+1597)s+987.1597} \end{aligned}$$

In all the transfer functions, the coefficients of the characteristic polynomial are positive and there is no missing coefficient. These are the necessary RH criteria to be satisfied for stability. To test the sufficient condition we perform RH array analysis by calling `routh_t()` function in Scilab. This analysis for all transfer function shows positive array coefficients and no sign change of the coefficients. These results ensure overall stability of the transfer functions.

Now for over damped system, impulse response and step response are in equation (8) and (9) respectively.

$$v(t) = \frac{\omega_n}{2\sqrt{\zeta^2-1}}\left[e^{-(\zeta\omega_n-\omega_n\sqrt{(\zeta^2-1)}.t} - e^{-(\zeta\omega_n+\omega_n\sqrt{(\zeta^2-1)}.t}\right] \tag{8}$$

which approaches a Dirac Delta function and decays to a steady state exponentially and

$$v(t) = 1-\frac{1}{2}\left[1+\frac{\zeta}{\sqrt{\zeta^2-1}}\right]e^{-(\zeta\omega_n-\omega_n\sqrt{(\zeta^2-1)}.t} + \frac{1}{2}\left[\frac{\zeta}{\sqrt{\zeta^2-1}}-1\right]e^{-(\zeta\omega_n+\omega_n\sqrt{(\zeta^2-1)}.t} \tag{9}$$

which rises to its peak without oscillation but a bit slower than critically damped oscillation. The responses, with $\zeta = 1.029085$ reduces respectively to

$$\begin{aligned} v_{im}(t) &= \frac{\omega_n}{0.486}\left[e^{-(1.029085.\omega_n-0.243\omega_n.)t} - e^{-(1.029085.\omega_n+0.243\omega_n).t}\right] \\ v_{im}(t) &= \frac{\omega_n}{0.486}\left[exp(-0.786\omega_n.t) - exp(-1.727\omega_n.t)\right] \end{aligned} \tag{10}$$

and

$$\begin{aligned} v_{step}(t) &= 1-2.62e^{-(1.029085\omega_n-0.243\omega_n).t} + 1.61e^{-(1.029085.\omega_n+0.243\omega_n.)t} \\ v_{step}(t) &= 1-2.62exp(-0.786\omega_n.t) + 1.61exp(-1.727\omega_n.t) \end{aligned} \tag{11}$$

The expression of cut off frequency from equation (4) is now stands as

$$\begin{aligned} \omega_c &\approx \omega_n \times 0.6180344 \\ \omega_c &\approx \sqrt{fib1.fib2} \times 0.6180344 \end{aligned} \tag{12}$$

The responses are graphically shown in figure (1). The step responses reach their respective peaks

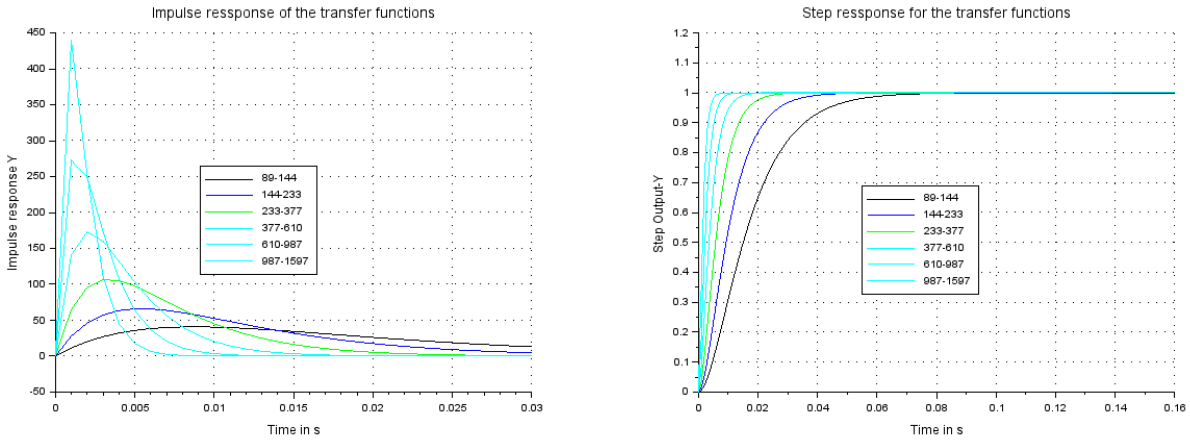

(a) Impulse responses

(b) Step responses

Figure 1: Impulse and step Responses of the transfer functions

without oscillation and without overshoot as described and the impulse responses decay to their minimum values exponentially and approaches the Dirac delta function with narrower width with increase of Fibonacci order. These plots verify the analytical results for over-damped oscillation. The magnitude variation of the transfer functions with frequency is shown in figure (2) All plots are flat similar to low pass filter. Obviously such flat, no spike response is observed in Butterworth and Bessel configurations. The theoretical cut offs and simulation results are summarize in the table (1). The z-value hypothesis testing is also shown in the table. Gain margin and phase margin are also calculated

Fib. No.	Cut-off frequency from (in rad/s)		Settling time(s)	Rise time(s)	z-value
	Analysis	Simulation			
$89, 144$	69.96	73.14 ± 4.27	0.05323	0.035751	0.747
$144, 233$	113.24	116.03 ± 5.78	0.032898	0.022096	0.483
$233, 377$	183.16	188 ± 11.04	0.020332	0.013656	0.438
$377, 610$	296.37	308.33 ± 19.10	0.012566	0.008440	0.626
$610, 987$	479.55	501.20 ± 30.79	0.007766	0.005216	0.697
$987, 1597$	775.93	805.37 ± 40.23	0.004800	0.003223	0.731

Table 1: Table for simulation data

with Scilab as ∞ since the phase response never crosses $-180\,\text{deg}$ and overshoot is nil for all T(s)s. Settling time and rise time are very small. Moreover for all the transfer functions, as usual represent over damped system.

A comparison with the established configurations with flat-response i.e. Butterworth and Bessel configuration is shown in the table (2)

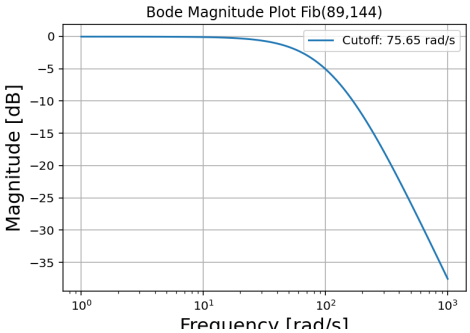

(a) for 89,144

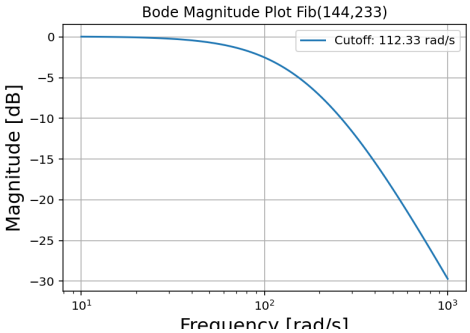

(b) for 144,233

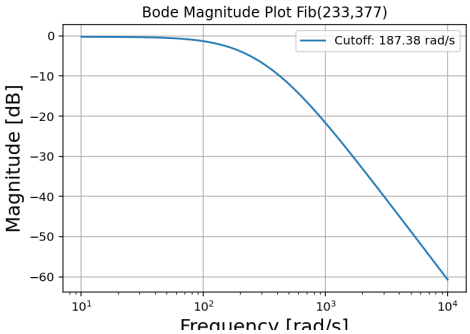

(c) for 233,377

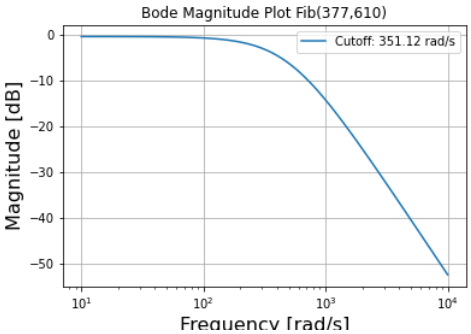

(d) for 377 610

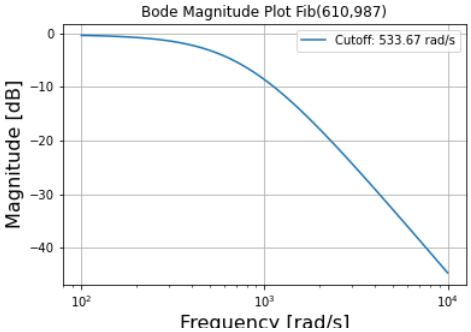

(e) for 610 987

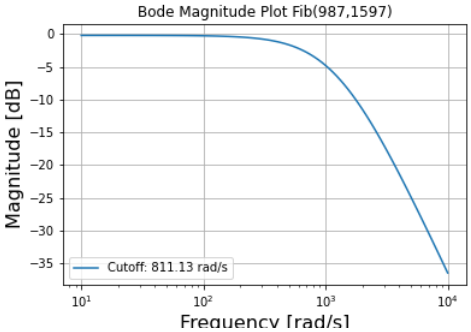

(f) for 987 1597

Figure 2: Bode plots of the transfer functions (Angular frequency – magnitude)

Quantity	Fibonacci-based	Butterworth	Bessel
Damping ratio ζ	1.029085	0.707	0.866
Magnitude response	flat	flat	flat
Nature	over damped	under damped	under damped
Phase response	non linear	non linear	linear
Overshoot	nil	present	present

Table 2: Comparison with established systems

5. Discussion

The systems we have designed are always stable in terms of pole position. Their gain & phase margin are infinite and hence can used to design system with higher gain without going the system to instability. They show slightly over damped characteristics resulting zero overshoot but slightly slower in response. The settling time & rise time are very small for all and as we extend our study to Fibonacci pairs from $(21-34)$ to $(46368-75015)$ we observe the decreasing trend of both the quantities.

On comparing with established systems, we found that the flat response of the designed system are similar to response of low pass Butterworth and Bessel configurations. Naturally the Butterworth configuration produces under damped oscillation and picks up peaks near the corner frequency when used for higher gain and higher order. The advantage of our designed ones are that such system dampen the possible blow up near the corner frequency. Moreover, there is no linear phase(ϕ) relationship with frequency(ω) as observed in Bessel configuration.

The cut of frequency of the systems calculated analytically lie within the single standard deviation of the population of cut offs calculated by simulation. The z-score of each pairs, shown in the table (1) establishes with 95% of confidence level that the analytically calculated cut off frequency is the cut off frequency of the transfer functions.

The transfer functions can be used to design low pass analog active filter with predictable cut off frequency and control system that requires no oscillation, no overshoot at the out put of step input.

6. Conclusion

The 2nd order open loop linear time invariant (LTI) systems designed from Fibonacci sequence have characteristics of low pass active filter transfer function that have flat response,over damped in nature and are always stable from all aspects.The LTI systems are represented by

$$T(s) = \frac{\omega_n^2}{s^2 + 2 \times 1.029\omega_n s + \omega_n^2} \tag{13}$$

with $\omega_n = \sqrt{fib1 \times fib2}$ and $\frac{fib2}{fib1} \approx 1.618$. The cut off frequencies are predictable from Fibonacci numbers as

$$\omega_c = \sqrt{fib1 \times fib2} \times 0.6180344$$

References

[1] C. S. Anil.D. Chavan, Correlation of fibonacci sequence and golden ratio with its applications in engineering and science, International Journal of Engineering and Management Research 6 (9) (2020) 07–14.

[2] S. Sinha, The fibonacci numbers and its amazing applications, International Journal of Engineering Science Invention 6 (9) (2017) 07–14.

[3] A. S. Pradip Kumar Sah1, Akanksha Madhuri Raj, Fibonacci sequence and golden ratio and its application, International Journal of Mathematics Trends and Technology 66 (3) (2020) 28–32.

[4] A. K. Pandey, S. Kanchan, A. K. Verma, Applications of fibonacci sequences and golden ratio, Journal of Informatics Electrical and Electronics Engineering 4 (1) (2023) 1–11.

[5] E. Çokduygulular, Fibonacci fractal-based optical filter design using zno/mgf_2 photonic crystals, Applied Physics Letters 116 (12) (2025) 1210–1215.

[6] A. Capponi, Expressing stochastic filters via number sequences, Applied Mathematics and Computation 217 (2010) 8267–8278.

[7] H. Tran-Ngoc, A promising approach using fibonacci sequence-based optimization algorithms for structural health monitoring, Scientific Reports 13 (2023) 4567.

[8] R. M. Abd-Elhameed, N. H. Alqubori, New expressions for polynomials combining fibonacci and lucas numbers, Journal of Applied Mathematics 58 (2024) 1023–1037.

[9] K. Mougkogiannis, On the response of proteinoid ensembles to fibonacci sequence stimuli, Bioelectronic Materials 7 (1) (2025) 89–99.

[10] P. Sudha, Application of fibonacci square in fashion design, International Journal of Analytical and Experimental Modal Analysis 12 (2) (2020) 2513–2515.

[11] The Interaction Design Foundation, The golden ratio - principles of form and layout, available at: `https://www.interaction-design.org/literature/article/the-golden-ratio-principles-of-form-and-layout` (2025).

[12] K. Bingi, R. Ibrahim, M. N. Karsiti, S. M. Hassan, V. R. Harindran, Design and analysis of fractional-order filters using scilab, in: 2018 IEEE 4th International Symposium in Robotics and Manufacturing Automation (ROMA), IEEE, 2018, pp. 1–6.

[13] S. F. Hussin, G. Birasamy, Z. Hamid, Design of butterworth band-pass filter, Politeknik & Kolej Komuniti Journal of Engineering and Technology 1 (1) (2016) 32–46.

[14] Z. M. M. Myo, Z. M. Aung, Z. M. Naing, Design and implementation of active band-pass filter for low frequency rfid (radio frequency identification) system, in: Proceedings of the International MultiConference of Engineers and Computer Scientists, Vol. 1, 2009, pp. 18–20.

[15] D. A. B. Vargas, R. F. Escobar, R. G. Suarez, Design of an active band-pass filter for the analysis of electromyographic signals derived from the median nerve, using genetic algorithms, International Journal of Applied Engineering Research 16 (7) (2021) 552–562.

[16] Y.-H. Chun, J.-R. Lee, S.-W. Yun, J.-K. Rhee, Design of an rf low-noise bandpass filter using active capacitance circuit, IEEE transactions on microwave theory and techniques 53 (2) (2005) 687–695.

[17] A. Sen, A. Das, J. Das, Software based pole zero extraction technique for analog filter and circuits, PREPARE@ u®| General Preprint Services (2019).

[18] X. W. Fuxian Chen, Qiuhui Chen, Filter banks from the fibonacci sequence, Pure and Applied Mathematics Journal Volume III,Issue VI (2019) 100–105.